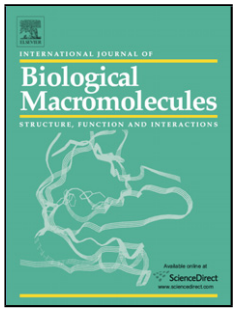

Title: Magnetic Stimuli-Responsive Chitosan-based Drug Delivery Biocomposite for Multiple Triggered Release

Author: Michael Harris Hamza Ahmed Brandico Barr David LeVine Leslie Pace Ankita Mohapatra Bashir Morshed PhD Joel D. Bumgardner PhD Jessica Amber Jennings PhD

PII: S0141-8130(16)32946-4
DOI: http://dx.doi.org/doi:10.1016/j.ijbiomac.2017.03.141
Reference: BIOMAC 7307

To appear in: *International Journal of Biological Macromolecules*

Received date: 21-12-2016
Revised date: 16-2-2017
Accepted date: 25-3-2017

Please cite this article as: M. Harris, H. Ahmed, B. Barr, D. LeVine, L. Pace, A. Mohapatra, B. Morshed, J.D. Bumgardner, J.A. Jennings, Magnetic Stimuli-Responsive Chitosan-based Drug Delivery Biocomposite for Multiple Triggered Release, *International Journal of Biological Macromolecules* (2017), http://dx.doi.org/10.1016/j.ijbiomac.2017.03.141

Title:

Magnetic Stimuli-Responsive Chitosan-based Drug Delivery Biocomposite for Multiple Triggered Release

Authors:

Michael Harris[a], Hamza Ahmed[a], Brandico Barr[a], David LeVine[a], Leslie Pace[a], Ankita Mohapatra[b], Bashir Morshed, PhD[b], Joel D. Bumgardner, PhD[a], Jessica Amber Jennings, PhD[a]

Institutions:

[a]Department of Biomedical Engineering; [b]Department of Electrical Engineering

The University of Memphis

3796 Norriswood Ave

Memphis TN, 38152

United States of America

Corresponding author:

Michael Harris

mhrris18@memphis.edu

Engineering Technology Room 330

3796 Norriswood Ave

Memphis TN, 38152 United States of America

Abstract

Stimuli responsive biomaterials offer a unique advantage over traditional local drug delivery systems in that the drug elution rate can be controllably increased to combat developing symptomology or maintain high local elution levels for disease treatment. In this study, superparamagnetic Fe_3O_4 nanoparticles and the antibiotic vancomycin were loaded into chitosan microbeads cross-linked with varying lengths of polyethylene glycol dimethacrylate. Beads were characterized using degradation, biocompatibility, and elution studies with successive magnetic stimulations at multiple field strengths and frequencies. Thirty-minute magnetic stimulation induced a temporary increase in daily elution rate of up to 45% that was dependent on field strength, field frequency and cross-linker length. Beads degraded by up to 70% after 3 days in accelerated lysozyme degradation tests, but continued to elute antibiotic for up to 8 days. No cytotoxic effects were observed *in vitro* compared to controls. These promising preliminary results indicate clinical potential for use in stimuli-controlled drug delivery.

Keywords: drug delivery, stimuli responsive biopolymer, magnetic nanoparticles

1. Introduction

Local drug delivery devices are designed to release therapeutics at a site of injury or disease, and maintain high concentrations of drug at desired locations while limiting systemic concentrations and toxic side effects [1-3]. While superior to conventional intravenous or intramuscular drug delivery methods, these local systems are limited in that they typically follow first order release patterns that release a set amount of drug despite changing physiological conditions [4]. Elution or release rates will eventually drop below therapeutic levels, which is especially problematic for antibiotic delivery systems, as sub-minimum inhibitory concentrations of antibiotics can lead to antibiotic resistant strains of bacteria [5-7]. Stimuli responsive or "smart" delivery systems offer additional control over the spatial and temporal release of encapsulated drugs through use of passive or active stimuli to alter the delivery matrix characteristics [8-10]. Active stimuli include magnetic fields, electric fields, ultrasonic waves, light, and externally generated heat, all of which can be applied to supply an on-demand increase in drug concentration at the target site due to often reversible changes in material conformations, phases, or chemical states [11-16]. The ability to externally modulate elution kinetics makes active-stimuli responsive systems advantageous, as it gives clinicians additional control over local drug concentrations throughout the treatment period. The spatiotemporal control offered by stimuli responsive biomaterials is particularly advantageous in the treatment of cancer and infection, in which high levels of therapeutic drug are needed at the target site but can induce toxic effects if administered systemically [17-20].

Of the active stimuli, magnetic stimulation is advantageous due to ease of use and the ability to target carriers in deeper tissues [23]. Magnetically responsive delivery systems are loaded with

superparamagnetic nanoparticles (MNP) < 15 nm, typically iron oxide Fe_3O_4, that become magnetized under the influence of an externally applied magnet [23, 24]. MNP have effectively been functionalized and coated with biocompatible polymers to yield nanoscale core-shell structures [10], loaded into the center of liposomes [25], and incorporated into hydrogels [26]. Under magnetic stimulation, the incorporated MNP generate local hyperthermic conditions which can either be used to treat tumors or induce drug release by way of improved diffusion, increased polymer matrix permeability, or breaking of temperature-labile drug linkers [23]. Stimulation response magnitude may be dependent on the frequency and strength of magnetic stimulation, providing a means of fine-tuning drug release [24]. MNP have been used to induce hyperthermia for tumor therapy in several clinical studies, with stimulations tolerated for durations of 1 hour or more at field strengths of up to 6 mT in the pelvic region [27, 28] and 17 mT intracranially [29]. Many of these studies use the MFH300F AC magnetic field applicator (MagForce Nanotechnologies GmbH, Berlin) which is large enough to accommodate humans and can produce magnetic fields from 0-23 mT at 100 kHz. MNP loaded polymer matrices have also been used in stimuli responsive drug delivery studies, with high frequency alternating magnetic stimulation strengths ranging from as low as 4 mT [30] to as high as 100 mT [31].

We hypothesized that Fe_3O_4 MNP could be loaded into chitosan microbeads cross linked with polyethylene glycol dimethacrylate (PEGDMA) to create a magnetically responsive local drug delivery system for treatment of musculoskeletal infections secondary to orthopedic surgery or trauma. Microbeads were loaded with vancomycin, an antibiotic with strong activity against genus *Staphylococcus* bacteria that are highly prevalent in musculoskeletal infections. PEGDMA is available in molecular weights ranging from M_n = 198 g/mol to over M_n = 20, 000 g/mol. We further hypothesize that the chosen length of cross linker will have a direct effect on

polymeric structure of the beads, with potential implications drug elution properties and effects on cells. In the present study, chitosan microbeads cross linked with various lengths of PEGDMA were compared to determine what effects, if any, the length of polymer cross linker had on bead swelling, drug elution rate, responsiveness to magnetic stimulation, degradation properties, and cytocompatibility. The effects of various magnetic field strengths and field frequencies on drug elution rate were also assessed for beads made with M_n = 550 PEGDMA

2. Experimental

2.1.Materials

Chitopharm S chitosan powder with an 82.5 ± 1.7 degree of deacetylation and an average molecular weight of 250.6 kDA was purchased from Chitopharm (Tromsø, Norway). NIH 3T3 fibroblast cells were acquired from ATCC. Cellgro Dulbecco's modified eagle medium with L glutamine and sodium pyruvate (DMEM), fetal bovine serum, Normocin (Corning, Manassas VA) were purchased from Fisher Scientific. Concentrated phosphate buffered saline (PBS), mineral oil, and high performance liquid chromatography (HPLC) reagents (Fisher Scientific, Hampton, NH) were purchased from Fisher Scientific. CellTiter-Glo viability assays were purchased from Promega (Madison, WI). Lysozyme Type VI from chicken egg white was purchased from MP Biomedicals LLC (Solon, OH). Vancomycin and polyethylene glycol dimethacrylate (PEGDMA) M_n= 550 and M_n = 750 were purchased from Sigma Aldrich (St. Louis, MO). PEGDMA M_n = 200 and M_m = 600 were purchased from Polysciences (Warminster, PA).

2.2 Fabrication of microbeads

Fe_3O_4 MNP were made according to a previously developed protocol by Kang et al. [32]. Iron oxide (Fe_3O_4) and Iron chloride ($FeCl_3$) were dissolved in HCl at concentrations of 0.5M and slowly dropped into dilute sodium hydroxide at pH 11-12. MNP were washed several times with HCL and deionized water prior to use. Previous imaging has shown the MNP average diameter to be approximately 10.89±2.67 nm. Each batch of MNP was characterized using x-ray diffraction (D8 Advance, Bruker Corporation, Billerica, MA) to ensure consistency. One gram of MNP was sonicated in 47 mL DI water for 1 hour to ensure even MNP distribution. There was no significant temperature increase. Two grams of chitosan powder, 400 mg vancomycin and 0.5 mL glacial acetic acid was then added and mixed by hand. The solution was stirred using a non-magnetic overhead impeller for 24 hours. The microbeads were then fabricated using a water in oil emulsion process. The oil solution consisted of 75 mL light mineral oil, 75 mL heavy mineral oil, 15 mL of the appropriate PEGDMA cross-linker and 2g Span 80 surfactant. The oil solution was stirred using a separate impeller and heated to 37° C. Fifteen mL of the chitosan-MNP-vancomycin solution was slowly added to the stirring oil using a 30-mL syringe. The solution was slowly heated to 60° C and allowed to stir for 24 hours. The beads were then washed to remove oil, surfactant and excess PEGDMA using a vacuum flask and successive treatment with hexanes, methanol, and acetone. The beads were then collected, weighed, and put into vials for the separate experiments.

2.3 Imaging

Beads were attached to stubs by adhesive carbon backing and then sputter coated with a Gold/Palladium (80:20) thin film approximately 20nm thick. A field emission scanning electron microscope (Nova NanoSEM 650, FEI, Hillsboro, Oregon) was used to image chitosan-

PEGDMA M_n = 550 beads with MNP. ImageJ (National Institute of Health, Bethesda, Maryland) was used to determine bead diameter.

2.4 Swelling ratio

50 mg of chitosan microbeads with each length of PEGDMA cross-linker were placed in 5 mL tubes with 2 mL of PBS at room temperature (n=3). After 24 hours, PBS was drained and excess liquid was removed using Kimwipes™ (Kimberly-Clark Kimetch, Irving, Texas). Samples were then immediately reweighed [33, 34]. Swelling ratio was determined as a percent increase in mass after immersion in PBS.

$$\text{Swelling ratio} = \frac{\text{weight after soaking}}{\text{initial dry weight}} \times 100\%$$

2.5 Elution and stimulation

To determine *in vitro* elution patterns, 2 mL of PBS were added to 50 mg of beads (n=4) at room temperature, with groups for each length of cross-linker and four additional groups with only PEGDMA M_n=550 to test the effects of field strength and field frequency (Table 1). Sampling occurred every 24 hours with complete media refreshment for 8 days. Each group was subjected to 30 minutes of magnetic stimulation or sham stimulation on days 3, 5 and 7 using a MagneTherm™ magnetic field generator (NanoTherics, Newcastle, UK). All lengths of PEGDMA beads were stimulated at 23 mT and 109.9 kHz. To assess the effect of field strength, M_n = 550 beads were tested at 75% and 50% of the original 23 mT field strength (17 mT and 11mT respectively) at a field frequency of 109.9 kHz. Field frequency was also tested on M_n = 550 beads at frequencies of 109.9 kHz, 330.4 kHz and 524.8 kHz with a field strength of 17 mT. Small 25 μL samples were taken before and after stimulation to determine if vancomycin

concentration increased during this period. Total vancomycin release was estimated as the total amount of vancomycin eluted into PBS once the daily elution rate had dropped below 1% of the cumulative elution for that group. To estimate theoretical vancomycin loading, the estimated cumulative release value was divided by bead mass. Vancomycin concentration in eluate samples was determined using high performance liquid chromatography (Dionex UltiMate 3000 HPLC, Thermo Scientific, Waltham, MA) with a C18 150x4.6 mm column (Hypersil Gold, Thermo Scientific). HPLC mobile phase consisted of 70% (0.124M KH2PO4 and 0.08M K2HPO4) and 30% acetonitrile pumped at 1 mL/min [35]. Retention time was approximately 1.6 minutes.

2.6 Degradation

To determine the degradation profile of Chitosan-MNP beads, a 21-day degradation study was performed using beads cross-linked with M_n = 550 PEGDMA with time points at 3, 5, 7, 14 and 21 days. A 3-day elution study was performed using PEGDMA M_n = 200, M_n = 600 and M_n = 750 cross-linked beads to compare initial degradation rates. Each group included 3 bead samples per time point weighing 50 mg per sample. Ten mL of 1 mg/mL lysozyme in PBS were added to each test tube and replaced during every 48-hour interval to replenish the enzymes that promote degradation. Beads were incubated at 37° C under constant orbital shaking throughout the experiment. At the end of every time point, the lysozyme solution was removed, and the beads were washed twice with 20 mL of deionized water. The beads were placed in a vacuum oven at 50 °C and -20 PSI until no changes in weight occurred during daily re-weighing. At the end of each drying cycle the weight was recorded and the percentage remaining was calculated using the equation:

Percent Remaining (%) = (Final Sample Weight (mg))/ (Initial Sample Weight (mg)) × 100

2.7 Cytocompatibility

NIH3T3 fibroblast cells were seeded into 24 well flat bottom plates at a density of 1 x 10^4 cells/cm^2 in DMEM media supplemented with 10% fetal bovine serum (FBS) and 100 µg/mL Normocin^{TM} antibiotic/antimycotic. All cells were stored in a humid incubator at 37° C and 5% CO_2. After overnight attachment and observation, beads from each group were added to wells at concentrations of 5 and 10 mg/cm^2 of well plate surface area (n=4). Silicone beads were added at a density of 10 mg/cm^2 to serve as bioinert control beads. Four wells did not receive any beads and were used as positive cell growth controls. On day three, wells were imaged using an EVOS microscope (AMG, Washington) and ATP concentration, which is proportional to the number of metabolically active cells, was quantified compared to controls using CellTiter-Glo®. CellTiter-Glo was added to each well and the luminescence of the media/CellTiter-Glo solution was used to quantify ATP concentration [36, 37]. Measured values were normalized to the control group that did not receive beads.

2.8 Statistical Analysis

All statistical tests were performed using SigmaPlot software (Systat Software, San Jose, California). One-way ANOVA with a Holm-Sidak post-hoc analysis was used to detect differences in swelling ratio, degradation rate, stimulation response and cytocompatibility between groups with different cross-linkers. The three stimulations were treated as separate events due to expected decreases in elution rate and stimulation response magnitude with time. The level of significance was taken as $\alpha = 0.05$.

3. Results and Discussion

3.1.Characterization

SEM images show spherical beads with slightly porous outer surfaces (Fig. 1). The beads embedded with MNP were 210 ± 40 microns in diameter with dimples covering the entire area of the beads. Chitosan beads have been manufactured using a wide variety of fabrication techniques with bead sizes ranging from the nanoscale to several millimeters [38, 39]. Previous research on microbeads has shown that elution rate increases for beads with smaller diameters, likely as a result of a higher surface area to volume ratio [40]. This increased elution rate reduces the effective release duration from small beads, limiting their potential for infection treatment or prevention. The 200 μm diameter of the beads used in this study is a compromise between achieving prolonged elution duration while still being small enough to fill irregularly shaped wound beds.

3.2 Swelling Ratio

Beads from all groups swelled to at least twice their original size (Fig. 2), with no clear trend between cross-linker size and swelling ratio. Beads cross-linked with M_n = 550 PEGDMA swelled to 300% of their original size, which is statistically higher than beads cross linked with M_n = 200, M_n = 600 or M_n = 750 PEGDMA ($p < 0.001$). Beads cross-linked with M_n = 200 PEGDMA swelled significantly more than M_n = 600 and M_n = 750 beads ($p = 0.01$). However, there were no significant differences between the 600 and 750 groups ($p > 0.5$). It was anticipated that the shortest cross linker in the study, M_n = 200 PEGDMA, would produce highly cross linked beads with low swelling ratios, while higher molecular weights would result in fewer chitosan-PEGDMA bonds and a more flexible polymer matrix. The increase in swelling ratio for M_n = 550 cross-linker compared to M_n = 200 is comparable to the behavior of other cross-linked PEG hydrogels [44] but the larger M_n = 600 and M_n = 750 PEGDMA cross linked beads allowed less water influx than expected. Results suggest that the size of PEGDMA

molecules with M_n above 550 may limit the number of PEG molecules that are incorporated within a bead, which may result in varying degrees of cross-linking densities, primary chain cyclization (PEGDMA chains crosslinking within the molecule), or drug molecule binding [45, 46].

3.3 Elution and Stimulation

Data shows that all groups eluted vancomycin in a burst-release pattern over the first 2-3 days, with exponential decrease in release over the remainder of the 8-day elution study (Fig. 3). Beads cross-linked with M_n = 600 PEGDMA eluted 33% more vancomycin on day 1 and 81% more vancomycin on day 2 compared to the cross-linker group with the next highest elution rate ($p < 0.001$). Beads cross-linked with M_n = 550 PEGDMA had higher mean elution rates on days 3-8 in the stimulated group and days 5-8 in the control group, however differences were not statistically significant ($p > 0.05$). Cumulative vancomycin release per 50 mg of beads ranged from 1.7 mg to 3.5 mg, with M_n = 600 beads releasing more vancomycin than the other cross linker groups (Table 2, $p < 0.001$). Beads cross linked with M_n = 550 PEGDMA eluted significantly more vancomycin than M_n = 750 beads ($p < 0.001$), although the increase over M_n = 200 beads was not significant ($p = 0.31$).

The M_n = 550 PEGDMA group had a significantly higher stimulus response than other crosslinker groups, with a 94 μg/ml increase during the first stimulation period that resulted in an overall 45% increase in day 3 elution compared to nonstimulated control samples ($p < 0.01$)., This is not surprising given the swelling ratio data, which shows that the M_n = 550 beads undergo larger changes in volume than beads cross-linked with other lengths of PEGDMA. It can be reasoned that any stimulation induced hyperthermia or matrix permeability increases would cause a greater effect in these beads due to increased matrix flexibility. One way ANOVA

was unable to detect significant differences between control and stimulated groups during the third stimulation period, but eluate samples from the M_n = 550 beads showed a 20% increase in vancomycin concentration during this period (Fig. 4A). Responsiveness to three separate stimulation periods suggests that any MNP-hyperthermia induced changes are temporary and dissipate when the magnetic field is removed.

There was a statistically significant increase of approximately 100 µg/mL vancomycin from beads stimulated at 17 mT and 23 mT compared to 11 mT at day 3 ($p < 0.001$, Fig. 4B). There was also an increase of approximately 30 µg/ml from beads stimulated at 17 mT and 23 mT on day 5, which was statistically higher than controls and beads stimulated at 11 mT ($p = 0.01$). These findings agree with studies showing diclofenac release from MNP-loaded chitosan carrageenan cross-linked with iron salts increase in response to higher magnetic fields [47], although not in a linear fashion for the tested range of field strengths. Beads subjected to 109.9 kHz stimulation eluted more vancomycin during the first stimulation at 107 µg/mL, compared to 65 µg/mL and 64 µg/mL for beads stimulated at 330.4 kHz and 524.8 kHz, respectively, however the number of samples was not great enough to detect statistical significance (Figure 4C, $p = 0.2$).

The ability to modulate vancomycin release with separate stimulations is advantageous compared to other smart delivery systems. Magnetoliposomes are another externally tunable drug delivery system, but rapidly release the complete drug payload as the MNP heats the surrounding lipids beyond its phase transition temperature [48]. Drug release from pH responsive nanogels follows a similar pattern, eluting most of the drug payload within 24 hours of exposure to acidic solutions [49]. Drug elution from chitosan-PEGDMA microbeads can be controllably increased using external magnetic field stimulation but, unlike many smart delivery systems, the

beads will still retain enough drug to continue delivering therapeutic doses for extended periods. This is especially beneficial in the treatment of bacterial infections, which require prolonged treatment with high concentrations of antibiotics.

3.4 Degradation

Local drug delivery devices should be consistently and functionally biodegradable to avoid issues such as buildup of degradation byproducts, rapid elution of drug payload, or future bacterial seeding after drug delivery is complete. According to results, 70 % (±1%) of degradation in the M_n = 550 PEGDMA group takes place within the first three days of the degradation period (Fig. 5A). After the first three days of the degradation period, there seemed to be no significant change in the degradation profile of Chitosan-PEGDMA MNP-loaded chitosan microbeads. When the microbeads were compared to cross-linkers with different molecular weights, there was a trend towards increased degradation rate for increasing molecular weight of PEGDMA cross-linker (Fig. 5B), with statistically significant differences in degradation rate between all groups ($p < 0.01$) with the exception of M_n = 600 and M_n = 750 beads ($p = 0.17$).

Lysozyme is known to be found in various bodily tissues, including serum in concentrations ranging from 1 to 14 μg/mL [50, 51], in contrast to the 1 mg/mL concentration used in this study. An elevated concentration was chosen for comparison with previous studies [52-54], although this likely results in accelerated degradation times compared to *in vivo* use. Lysozyme breaks chitosan down by cleaving the (β 1→4) glycosidic bonds between polysaccharide units in the polymer leaving glucosamine byproducts that are incorporated into proteoglycans or metabolized by the body [55]. Approximately 30% of the microbead composition consisted of MNP therefore, the degradation profile suggests that the majority of the chitosan-PEGDMA composite

had degraded entirely by day 3 in this accelerated degradation study. Up to 80% of initial weight was retained after elution studies in PBS without lysozyme, suggesting that enzymatic degradation by lysozyme is the predominant mechanism measured in this evaluation. This would likely mean a prolonged degradation time when implants are placed *in vivo* since elevated lysozyme concentrations were used in this accelerated test. In vivo degradation studies are needed to adequately determine timing of degradation response.

PEG hydrogels typically have similar or slower degradation rates to those in our study [45, 56, 57]. The enzyme-cleavable chitosan backbone for PEG cross-linked beads may provide a means to tailor degradation to match needs based on drug elution or tissue in-growth rates [58]. In studies of other forms of cross-linked chitosan microbeads, little or no degradation of composites is observed over the course of weeks, both *in vitro* and *in vivo* [34, 59, 60], which may limit the utility for a local drug delivery system. Systems that undergo no or little degradation can serve as a scaffold for hematogenous bacterial attachment after drug delivery is completed, increasing the risk of infection compared to the degradable beads presented in this study.

3.5 Cytocompatibility

Cells exhibited normal spindle shaped morphologies when exposed to either silicone or vancomycin loaded chitosan-PEGDMA beads (Fig. 6). Cellular metabolism ranged from 97% to 152% for groups with MNP-loaded microbeads added (Fig. 7). There was a significant increase in ATP concentration for samples treated with MNP beads at a concentration of 5 mg/mL ($p<0.001$), but no increase in ATP concentration for samples that received non-MNP beads ($p = 0.77$). The results from the metabolism assay confirm visual microscopic observations that both Si and MNP beads showed high compatibility with cells.

Both chitosan and PEG have favorable biocompatibility properties and should not have a negative effect on cellular proliferation or metabolism [61-64]. Vancomycin is a commonly used antibiotic with no reported effects on fibroblast growth at concentrations up to 1 mg/ml [65]. The iron oxide within microbeads may play a role in the increased viability for the lower concentration of MNP-loaded microbeads, showing similar findings to a study by Berry et al. in which bare iron oxide nanoparticles caused decreased viability but showed a 33% increases when modified with the protein albumin [66]. Hydrogels of PEG and PEG blended with chitosan that use photoinitiated PEGDMA or PEG diacrylate have been used to successfully entrap cells and support cell viability [67, 68]. High percent cell viability may also indicate that residual unbound PEGDMA is removed during the wash steps, as unreacted methacrylates have known toxicity to fibroblasts and other cells [69-71]. Further evaluation of tissue response to MNP-loaded chitosan-PEG microspheres should include evaluation of immune cell activation as well as in vivo implantation.

4. Conclusion

In this preliminary study, it was shown that MNP loaded chitosan microbeads cross-linked with PEGDMA are capable of releasing vancomycin for up to 8 days. Short 30-minute magnetic stimulations can significantly increase daily drug elution rate up to 45% in beads cross linked with M_n = 550 PEGDMA ($p < 0.01$), likely via a temporary increase in permeability due to MNP generated hyperthermia. The polymer matrix is rapidly biodegradable and shows no signs of significant cytotoxicity against fibroblast cells *in vitro*. The ability to increase drug elution on demand makes these beads appealing as a potential infection prevention and treatment device, as magnetic stimulation can be used to either increase drug delivery post-implantation for maximum drug concentration or maintain therapeutic drug levels after traditional delivery

systems would have fallen below the desired elution rate. Further extension of these drug delivery matrices to release of proteins, small molecules, or other chemotherapeutics may prove useful in a wide-range of clinical applications, such as tissue regeneration, pain relief, and cancer treatment. Ongoing studies will continue to evaluate the effect of general hyperthermia on vancomycin release, effect of MNP loading concentration on bead responsiveness, effects of additional stimulation parameters such as duration and number of stimulations, characterize the bead polymer matrix, and test *in vivo* efficacy.

Acknowledgements

Funding: This work was supported by the Fed Ex Institute of Technology Innovation Grant (2012-537865) and the University of Memphis Helen Hardin Honors Program. We would also like to thank Dr. Warren Haggard for laboratory supplies in addition to project and experimental guidance, Dr. Tomiko Fujiwara for advice in selecting the PEGDMA cross-linker, and both Madhav Ghimire and Dr. Sanjay Mishra for providing the MNP for this project.

References

[1] C.G. Zalavras, M.J. Patzakis, P. Holtom, Local antibiotic therapy in the treatment of open fractures and osteomyelitis, Clinical orthopaedics and related research 427 (2004) 86-93.

[2] M.E. Hake, H. Young, D.J. Hak, P.F. Stahel, E.M. Hammerberg, C. Mauffrey, Local antibiotic therapy strategies in orthopaedic trauma: Practical tips and tricks and review of the literature, Injury 46(8) (2015) 1447-1456.

[3] M. El-Husseiny, S. Patel, R. MacFarlane, F. Haddad, Biodegradable antibiotic delivery systems, Bone & Joint Journal 93(2) (2011) 151-157.

[4] Y. Fu, W.J. Kao, Drug release kinetics and transport mechanisms of non-degradable and degradable polymeric delivery systems, Expert opinion on drug delivery 7(4) (2010) 429-444.

[5] M. Bassetti, M. Merelli, C. Temperoni, A. Astilean, New antibiotics for bad bugs: where are we?, Ann. Clin. Microbiol. Antimicrob. 12 (2013) 22.

[6] P.S. Stewart, J.W. Costerton, Antibiotic resistance of bacteria in biofilms, Lancet 358(9276) (2001) 135-8.

[7] I.M. Gould, Antibiotic resistance: the perfect storm, Int. J. Antimicrob. Agents 34 Suppl 3 (2009) S2-5.

[8] E. Fleige, M.A. Quadir, R. Haag, Stimuli-responsive polymeric nanocarriers for the controlled transport of active compounds: concepts and applications, Advanced drug delivery reviews 64(9) (2012) 866-84.

[9] P. Bawa, V. Pillay, Y.E. Choonara, L.C. du Toit, Stimuli-responsive polymers and their applications in drug delivery, Biomedical Materials 4(2) (2009).

[10] J. Zhang, R.D.K. Misra, Magnetic drug-targeting carrier encapsulated with thermosensitive smart polymer: Core-shell nanoparticle carrier and drug release response, Acta Biomater. 3(6) (2007) 838-850.

[11] J.L. Paris, M.V. Cabanas, M. Manzano, M. Vallet-Regi, Polymer-Grafted Mesoporous Silica Nanoparticles as Ultrasound-Responsive Drug Carriers, ACS nano 9(11) (2015) 11023-33.

[12] T. Neuberger, B. Schopf, H. Hofmann, M. Hofmann, B. von Rechenberg, Superparamagnetic nanoparticles for biomedical applications: Possibilities and limitations of a new drug delivery system, Journal of Magnetism and Magnetic Materials 293(1) (2005) 483-496.

[13] S. Giri, B.G. Trewyn, M.P. Stellmaker, V.S.Y. Lin, Stimuli-responsive controlled-release delivery system based on mesoporous silica nanorods capped with magnetic nanoparticles, Angewandte Chemie-International Edition 44(32) (2005) 5038-5044.

[14] C. Alvarez-Lorenzo, L. Bromberg, A. Concheiro, Light-sensitive Intelligent Drug Delivery Systems, Photochem. Photobiol. 85(4) (2009) 848-860.

[15] F. Movahedi, R.G. Hu, D.L. Becker, C. Xu, Stimuli-responsive liposomes for the delivery of nucleic acid therapeutics, Nanomedicine: Nanotechnology, Biology and Medicine 11(6) (2015) 1575-1584.

[16] S. Ganta, H. Devalapally, A. Shahiwala, M. Amiji, A review of stimuli-responsive nanocarriers for drug and gene delivery, Journal of controlled release 126(3) (2008) 187-204.

[17] G. Kahlmeter, J.I. Dahlager, Aminoglycoside toxicity - a review of clinical studies published between 1975 and 1982, The Journal of antimicrobial chemotherapy 13 Suppl A (1984) 9-22.

[18] G.R. Bailie, D. Neal, Vancomycin ototoxicity and nephrotoxicity. A review, Med. Toxicol. Adverse Drug Exp. 3(5) (1988) 376-86.

[19] T. al-Tweigeri, J.M. Nabholtz, J.R. Mackey, Ocular toxicity and cancer chemotherapy. A review, Cancer 78(7) (1996) 1359-73.

[20] J. Khatcheressian, T.J. Smith, Review: adding cytotoxic drugs to a chemotherapy regimen increases tumor response rates and toxicity, but not survival in metastatic breast cancer, ACP J. Club 146(1) (2007) 5.

[21] D.E. DeWitt, I.B. Hirsch, Outpatient insulin therapy in type 1 and type 2 diabetes mellitus: scientific review, JAMA 289(17) (2003) 2254-64.

[22] A.J. Hahr, M.E. Molitch, Optimizing insulin therapy in patients with type 1 and type 2 diabetes mellitus: optimal dosing and timing in the outpatient setting, Am. J. Ther. 15(6) (2008) 543-50.

[23] C.S. Kumar, F. Mohammad, Magnetic nanomaterials for hyperthermia-based therapy and controlled drug delivery, Advanced drug delivery reviews 63(9) (2011) 789-808.

[24] P. Bawa, V. Pillay, Y.E. Choonara, L.C. Du Toit, Stimuli-responsive polymers and their applications in drug delivery, Biomedical materials 4(2) (2009) 022001.

[25] M. Gonzales, K.M. Krishnan, Synthesis of magnetoliposomes with monodisperse iron oxide nanocrystal cores for hyperthermia, Journal of Magnetism and Magnetic Materials 293(1) (2005) 265-270.

[26] L. Lao, R. Ramanujan, Magnetic and hydrogel composite materials for hyperthermia applications, Journal of materials science: Materials in medicine 15(10) (2004) 1061-1064.

[27] M. Johannsen, U. Gneveckow, L. Eckelt, A. Feussner, N. Waldöfner, R. Scholz, S. Deger, P. Wust, S. Loening, A. Jordan, Clinical hyperthermia of prostate cancer using magnetic nanoparticles: presentation of a new interstitial technique, International journal of hyperthermia 21(7) (2005) 637-647.

[28] P. Wust, U. Gneveckow, M. Johannsen, D. Böhmer, T. Henkel, F. Kahmann, J. Sehouli, R. Felix, Magnetic nanoparticles for interstitial thermotherapy–feasibility, tolerance and achieved temperatures, International journal of hyperthermia 22(8) (2006) 673-685.

[29] K. Maier-Hauff, R. Rothe, R. Scholz, U. Gneveckow, P. Wust, B. Thiesen, A. Feussner, A. von Deimling, N. Waldoefner, R. Felix, Intracranial thermotherapy using magnetic nanoparticles combined with external beam radiotherapy: results of a feasibility study on patients with glioblastoma multiforme, Journal of neuro-oncology 81(1) (2007) 53-60.

[30] N.S. Satarkar, J.Z. Hilt, Magnetic hydrogel nanocomposites for remote controlled pulsatile drug release, Journal of controlled release 130(3) (2008) 246-251.

[31] S. Rana, A. Gallo, R. Srivastava, R. Misra, On the suitability of nanocrystalline ferrites as a magnetic carrier for drug delivery: functionalization, conjugation and drug release kinetics, Acta Biomaterialia 3(2) (2007) 233-242.

[32] Y.S. Kang, S. Risbud, J.F. Rabolt, P. Stroeve, Synthesis and characterization of nanometer-size Fe3O4 and γ-Fe2O3 particles, Chemistry of Materials 8(9) (1996) 2209-2211.

[33] G. Pasparakis, N. Bouropoulos, Swelling studies and in vitro release of verapamil from calcium alginate and calcium alginate–chitosan beads, International journal of pharmaceutics 323(1) (2006) 34-42.

[34] F.-L. Mi, H.-W. Sung, S.-S. Shyu, C.-C. Su, C.-K. Peng, Synthesis and characterization of biodegradable TPP/genipin co-crosslinked chitosan gel beads, Polymer 44(21) (2003) 6521-6530.

[35] M.M.D.C. Vila, R.M. de Oliveira, M.M. Goncalves, M. Tubino, Analytical methods for vancomycin determination in biological fluids and in pharmaceuticals, Quimica Nova 30(2) (2007) 395-399.

[36] T.L. Riss, R.A. Moravec, A.L. Niles, H.A. Benink, T.J. Worzella, L. Minor, Cell viability assays, (2015).

[37] R. Hannah, M. Beck, R. Moravec, T. Riss, CellTiter-Glo™ Luminescent cell viability assay: a sensitive and rapid method for determining cell viability, Promega Cell Notes 2 (2001) 11-13.

[38] X. Shu, K. Zhu, Controlled drug release properties of ionically cross-linked chitosan beads: the influence of anion structure, International journal of pharmaceutics 233(1) (2002) 217-225.

[39] J.A. Jennings, J. Bumgardner, Chitosan Based Biomaterials, Woodhead Publishing2016.

[40] S. Desai, J. Perkins, B.S. Harrison, J. Sankar, Understanding release kinetics of biopolymer drug delivery microcapsules for biomedical applications, Materials Science and Engineering: B 168(1) (2010) 127-131.

[41] Y. Yuan, B.M. Chesnutt, G. Utturkar, W.O. Haggard, Y. Yang, J.L. Ong, J.D. Bumgardner, The effect of cross-linking of chitosan microspheres with genipin on protein release, Carbohydrate Polymers 68(3) (2007) 561-567.

[42] D.Y. Pratt, L.D. Wilson, J.A. Kozinski, Preparation and sorption studies of glutaraldehyde cross-linked chitosan copolymers, J. Colloid Interface Sci. 395 (2013) 205-11.

[43] L. Poon, L.D. Wilson, J.V. Headley, Chitosan-glutaraldehyde copolymers and their sorption properties, Carbohydrate Polymers 109 (2014) 92-101.

[44] S.A. Meenach, J.Z. Hilt, K.W. Anderson, Poly(ethylene glycol)-based magnetic hydrogel nanocomposites for hyperthermia cancer therapy, Acta Biomater. 6(3) (2010) 1039-1046.

[45] S.J. Bryant, K.S. Anseth, Hydrogel properties influence ECM production by chondrocytes photoencapsulated in poly (ethylene glycol) hydrogels, J. Biomed. Mater. Res. 59(1) (2002) 63-72.

[46] A. Metters, J. Hubbell, Network formation and degradation behavior of hydrogels formed by Michael-type addition reactions, Biomacromolecules 6(1) (2005) 290-301.

[47] G.R. Mahdavinia, H. Etemadi, F. Soleymani, Magnetic/pH-responsive beads based on caboxymethyl chitosan and κ-carrageenan and controlled drug release, Carbohydrate Polymers 128 (2015) 112-121.

[48] M. Babincova, P. Čičmanec, V. Altanerova, Č. Altaner, P. Babinec, AC-magnetic field controlled drug release from magnetoliposomes: design of a method for site-specific chemotherapy, Bioelectrochemistry 55(1) (2002) 17-19.

[49] J.Z. Du, T.M. Sun, W.J. Song, J. Wu, J. Wang, A Tumor- Acidity- Activated Charge-Conversional Nanogel as an Intelligent Vehicle for Promoted Tumoral- Cell Uptake and Drug Delivery, Angewandte Chemie International Edition 49(21) (2010) 3621-3626.

[50] B. Porstmann, K. Jung, H. Schmechta, U. Evers, M. Pergande, T. Porstmann, H.-J. Kramm, H. Krause, Measurement of lysozyme in human body fluids: comparison of various enzyme immunoassay techniques and their diagnostic application, Clinical biochemistry 22(5) (1989) 349-355.

[51] J. Hankiewicz, E. Swierczek, Lysozyme in human body fluids, Clinica chimica acta 57(3) (1974) 205-209.

[52] C. Yomota, T. Komuro, T. Kimura, Studies on the degradation of chitosan films by lysozyme and release of loaded chemicals, Yakugaku zasshi: Journal of the Pharmaceutical Society of Japan 110(6) (1990) 442-448.

[53] K.Y. Lee, W.S. Ha, W.H. Park, Blood compatibility and biodegradability of partially N-acylated chitosan derivatives, Biomaterials 16(16) (1995) 1211-1216.

[54] D. Ren, H. Yi, W. Wang, X. Ma, The enzymatic degradation and swelling properties of chitosan matrices with different degrees of N-acetylation, Carbohydrate Research 340(15) (2005) 2403-2410.

[55] T. Kean, M. Thanou, Biodegradation, biodistribution and toxicity of chitosan, Advanced drug delivery reviews 62(1) (2010) 3-11.

[56] J. Patterson, J.A. Hubbell, Enhanced proteolytic degradation of molecularly engineered PEG hydrogels in response to MMP-1 and MMP-2, Biomaterials 31(30) (2010) 7836-7845.

[57] B. Reid, M. Gibson, A. Singh, J. Taube, C. Furlong, M. Murcia, J. Elisseeff, PEG hydrogel degradation and the role of the surrounding tissue environment, J. Tissue Eng. Regen. Med. 9(3) (2015) 315-8.

[58] C.-C. Lin, K.S. Anseth, PEG hydrogels for the controlled release of biomolecules in regenerative medicine, Pharm. Res. 26(3) (2009) 631-643.

[59] B.T. Reves, J.D. Bumgardner, W.O. Haggard, Fabrication of crosslinked carboxymethylchitosan microspheres and their incorporation into composite scaffolds for enhanced bone regeneration, Journal of Biomedical Materials Research Part B: Applied Biomaterials 101(4) (2013) 630-639.

[60] S. Jameela, A. Jayakrishnan, Glutaraldehyde cross-linked chitosan microspheres as a long acting biodegradable drug delivery vehicle: studies on the in vitro release of mitoxantrone and in vivo degradation of microspheres in rat muscle, Biomaterials 16(10) (1995) 769-775.

[61] B. Carreño-Gómez, R. Duncan, Evaluation of the biological properties of soluble chitosan and chitosan microspheres, Int. J. Pharm. 148(2) (1997) 231-240.

[62] F.-L. Mi, Y.-C. Tan, H.-F. Liang, H.-W. Sung, In vivo biocompatibility and degradability of a novel injectable-chitosan-based implant, Biomaterials 23(1) (2002) 181-191.

[63] S. Lin-Gibson, S. Bencherif, J.A. Cooper, S.J. Wetzel, J.M. Antonucci, B.M. Vogel, F. Horkay, N.R. Washburn, Synthesis and characterization of PEG dimethacrylates and their hydrogels, Biomacromolecules 5(4) (2004) 1280-1287.

[64] T. Vermonden, R. Censi, W.E. Hennink, Hydrogels for protein delivery, Chem. Rev. 112(5) (2012) 2853-2888.

[65] J.K. Smith, A.R. Moshref, J.A. Jennings, H.S. Courtney, W.O. Haggard, Chitosan sponges for local synergistic infection therapy: a pilot study, Clinical Orthopaedics and Related Research® 471(10) (2013) 3158-3164.

[66] C.C. Berry, S. Wells, S. Charles, A.S. Curtis, Dextran and albumin derivatised iron oxide nanoparticles: influence on fibroblasts in vitro, Biomaterials 24(25) (2003) 4551-7.

[67] A. Escudero-Castellanos, B.E. Ocampo-Garcia, M.V. Dominguez-Garcia, J. Flores-Estrada, M.V. Flores-Merino, Hydrogels based on poly(ethylene glycol) as scaffolds for tissue engineering application: biocompatibility assessment and effect of the sterilization process, J. Mater. Sci. Mater. Med. 27(12) (2016) 176.

[68] W.G. Koh, A. Revzin, M.V. Pishko, Poly(ethylene glycol) hydrogel microstructures encapsulating living cells, Langmuir : the ACS journal of surfaces and colloids 18(7) (2002) 2459-62.

[69] L. Stanislawski, M. Lefeuvre, K. Bourd, E. Soheili-Majd, M. Goldberg, A. Perianin, TEGDMA-induced toxicity in human fibroblasts is associated with early and drastic glutathione depletion with subsequent production of oxygen reactive species, J. Biomed. Mater. Res. A 66(3) (2003) 476-82.

[70] B. Thonemann, G. Schmalz, K.A. Hiller, H. Schweikl, Responses of L929 mouse fibroblasts, primary and immortalized bovine dental papilla-derived cell lines to dental resin components, Dent. Mater. 18(4) (2002) 318-323.

[71] S. Krifka, G. Spagnuolo, G. Schmalz, H. Schweikl, A review of adaptive mechanisms in cell responses towards oxidative stress caused by dental resin monomers, Biomaterials 34(19) (2013) 4555-4563.

Table 1: Stimulation Parameters

PEGDMA molecular weight	Magnetic Field Strength	Magnetic Field Frequency
200	23 mT	109.9 kHz
550	23 mT	109.9 kHz
600	23 mT	109.9 kHz
750	23 mT	109.9 kHz
550	17 mT	109.9 kHz
550	11 mT	109.9 kHz
550	17 mT	330.4 kHz
550	17 mT	524.8 kHz
200	0 mT	N/A
550	0 mT	N/A
600	0 mT	N/A
750	0 mT	N/A

Table 2: Cumulative Vancomycin Release (mg)

PEGDMA Mn	Average Vancomycin release (mg)	Standard Deviation (mg)
200	2.36	0.25
550	2.48	0.31
600	3.52	0.14
750	1.69	0.2

Figure 1: SEM micrograph showing chitosan-PEGDMA M_n= 550 microbeads with MNP at 1000x magnification.

Figure 2: Graph shows swelling ratio of chitosan beads with various lengths of PEGDMA after 24 hours (n = 3). Mean ± standard deviation. * Represents statistical difference compared to 200 (* $p < 0.05$, ** $p < 0.01$). # Represents statistical difference compared to 550 (# $p < 0.05$, ## $p < 0.01$). & Represents statistical difference compared to 600 (& $p < 0.05$, && $p < 0.01$). † Represents statistical difference compared to 750 († $p < 0.05$, †† $p < 0.01$).

Figure 3: Graph shows the complete 8-day elution of (A) control and (B) stimulated groups for all lengths of PEGDMA cross-linker used in this study (n=4). Stimulations were performed on days 3, 5 and 7 with a field strength of 23 mT and frequency of 109.9 kHz. Mean ± standard deviation.

Comment [mh1]: color

Figure 4: Bar graphs compare the increase in vancomycin concentration during the three stimulation periods for A) various lengths of PEGDMA cross-linker (* Represents statistical difference compared to 200, # represents statistical difference compared to 550, & represents statistical difference compared to 600, † represents statistical difference compared to 750, $p < 0.05$), B) three magnetic field strengths (* Represents statistical difference compared to control, # represents statistical difference compared to 11 mT, & represents statistical difference compared to 17 mT, † represents statistical difference compared to 23 mT, $p < 0.05$), and C) three magnetic field frequencies. Mean ± standard deviation (n = 4 in all graphs)/

Comment [mh2]: color

Figure 5: A) Graph shows the 21-day degradation profile for beads cross-linked with Mn = 550 PEGDMA (n=3). B) A bar graph compares the three-day degradation of various chitosan beads cross-linked with various lengths of PEGDMA (n = 3). Mean ± standard deviation. * Represents

statistical difference compared to 200 (* $p < 0.05$, ** $p < 0.01$). # Represents statistical difference compared to 550 (# $p < 0.05$, ## $p < 0.01$). & Represents statistical difference compared to 600 (& $p < 0.05$, && $p < 0.01$). † Represents statistical difference compared to 750 († $p < 0.05$, †† $p < 0.01$).

Figure 6: Photomicrographs of NIH-3T3 cells growing (A) on control tissue culture plastic, (B) near silicone microparticles and C) near chitosan-PEGDMA $M_n = 550$ microbeads from the MNP Vanc 5 mg/mL group.

Figure 7: NIH-3T3 cell metabolism after 3 days exposure to chitosan-PEGDMA $M_n = 550$ microbeads with and without MNP and silicone microparticles (n = 4). Cell counts are normalized to control samples. Mean ± standard deviation. * Represents statistical difference in ATP concentration compared to control (* $p < 0.05$, ** $p < 0.01$).